**THE EUROPEAN
PHYSICAL JOURNAL B**

Regular Article

Hamilton-like statistics in onedimensional driven dissipative many-particle systems

M. Treiber[1] and D. Helbing[2,a]

[1] Institute for Economics and Traffic, Dresden University of Technology, Andreas-Schubert-Str. 23, 01062 Dresden, Germany
[2] ETH Zurich, UNO D11, Universitätstr. 41, 8092 Zurich, Switzerland

Abstract. This contribution presents a derivation of the steady-state distribution of velocities and distances of driven particles on a onedimensional periodic ring, using a Fokker-Planck formalism. We will compare two different situations: (i) symmetrical interaction forces fulfilling Newton's law of "actio = reactio" and (ii) asymmetric, forwardly directed interactions as, for example in vehicular traffic. Surprisingly, the steady-state velocity and distance distributions for asymmetric interactions and driving terms agree with the equilibrium distributions of classical many-particle systems with symmetrical interactions, if the system is large enough. This analytical result is confirmed by computer simulations and establishes the possibility of approximating the steady state statistics in driven many-particle systems by Hamiltonian systems. Our finding is also useful to understand the various departure time distributions of queueing systems as a possible effect of interactions among the elements in the respective queue [Physica A **363**, 62 (2006)].

PACS. 05.40.-a Fluctuation phenomena, random processes, noise, and Brownian motion – 05.10.Gg Stochastic analysis methods – 47.70.-n Reactive and radiative flows – 89.40.-a Transportation

1 Introduction

Classical many-particle systems such as ideal gases are characterized by the applicability of Newton's laws of mechanics, which particularly includes the law of "actio = reactio". With these basic laws, many fundamental properties can be derived, like the conservation of momentum and energy. Such many-particle systems are known as Hamiltonian systems. Even statistical physics and thermodynamics are based on these relationships.

But what would happen if the law of "actio = reactio" would not hold and the particle interactions would not fulfil momentum and energy conservation? Examples of such a system include granular flows [1] and driven Brownian particles, where many results for stationary distributions are available. However, interactions are taken into account only implicitly by a nonlinear friction function [2], or by a symmetric interaction potential [3]. In other systems such as vehicular traffic one would like to model the non-symmetric interactions between the particles (vehicles) explicitly. Would it still be possible to find (analytical) formulas for the stationary distributions of velocities and distances? In fact, although a statistical physics formalism for driven systems would be very desireable to have, there are still not many results available. The

existing results mainly concern the study of traffic-jam related condensation phenomena by means of the master equation [4] or the Fokker-Planck equation [5]. The related considerations have assumed certain arrival and departure rates to or from any forming vehicle clusters, but they have not explicitly represented the acceleration or deceleration dynamics of interacting vehicles in space and time, which is typically described in terms of microscopic traffic models [6]. In the following, we will take this dynamics of interacting particles into account.

In fact, we are seeking for a method to treat dissipative driven many-particle systems in a similar way as Hamiltonian systems. The idea is that the dissipation in the system would be balanced by the effect of the driving force, at least in a closed (circular) system and in the limit of large particle numbers. This idea has been used to evaluate the vehicle interaction potential [7–9], but questioned to be applicable to systems with asymmetric interactions. Moreover, the method has been restricted to a very limited number of potentials $U(s)$, as the normalization factor of the distance distribution could, in general, not be analytically determined.

For onedimensional classical Hamiltonian gases, many results have been previously derived in the framework of Random Matrix Theory [10,11]. According to this, if coupled to a thermal bath, the velocity distribution of gas

[a] e-mail: `dhelbing@ethz.ch`

particles is Gaussian and the distance distribution $g(s)$ can be written as

$$g(s) \propto e^{-[U(s)/\theta + Bs]}, \tag{1}$$

where $U(s)$ is the interaction potential, θ is the velocity variance (i.e. proportional to the temperature), and B depends on the particle density. It would be very desireable to have a similar result for driven many-particle systems, as this would allow one to determine the interaction potential and interaction force among driven particles in the presence of fluctuations. Our hope is that, in the stationary state, the dissipative interactions and the driving term would somehow cancel out on average, so that the behavior would actually correspond to a Hamiltonian-like system [12–14], as it was *presupposed* in references [8,9,11,15,16].

In fact, in this paper we will show that this idea is correct for onedimensional systems in the limit of large particle numbers. Even forwardly directed dissipative driven many-particle systems behave in a Hamiltonian-like way, if they are far enough away from dynamic instabilities.

Our paper is structured as follows: In the next section, we lay out the theoretical basis and derive the form of the onedimensional Hamiltonian as well as the conditions, under which it provides a correct description. In Section 3 we formulate the predictions in a form that can be tested by simulating representative many-particle systems. The actual simulations and their results are presented in Section 4, after which we conclude with a discussion.

2 Driven many-particle model with dissipative interactions

In the onedimensional driven-many particle system we discuss, point-like particles i change their location $x_i(t)$ in time t according to the equation of motion

$$\frac{dx_i}{dt} = v_i(t), \tag{2}$$

and their temporal velocity change dv_i/dt is assumed to be given by the following stochastic acceleration equation:

$$\frac{dv_i}{dt} = \frac{v_0 - v_i}{\tau} + f(s_i) - \gamma f(s_{i+1}) + \xi_i(t). \tag{3}$$

Here, v_0 denotes the "free" or "desired" velocity and $\xi_i(t)$ represents a white noise fluctuation term satisfying

$$\langle \xi_i(t) \rangle = 0,$$

$$\langle \xi_i(t)\xi_j(t') \rangle = D\delta_{ij}\delta(t - t'), \tag{4}$$

where D is a velocity-diffusion constant. The particle mass m_i has been set to 1, and $f(s_i) \leq 0$ describes a repulsive interaction force, which depends on the particle distance $s_i(t) = x_{i-1}(t) - x_i(t)$ where the particle index i increases in upstream direction. The term $\gamma f(s_{i+1})$ with $0 \leq \gamma \leq 1$

allows to study different cases: $\gamma = 1$ corresponds to the classical case of symmetrical interactions in forward and backward direction, fulfilling the physical law of "actio = reactio". $\gamma = 0$ corresponds to the case of forwardly directed interactions only, which is, for example, applicable to vehicles.

2.1 Fokker-Planck equation for velocities and distances

In this section, we will determine the statistical distributions of the velocities and distances of the N particles i. Rather than describing the dynamics by the above stochastic differential equation (Langevin equation), we will delineate it by an equivalent Fokker-Planck equation [17]. With the definitions

$$\mathbf{s} = (s_1, \ldots, s_N), \quad \mathbf{v} = (v_1, \ldots, v_N), \tag{5}$$

$$W(s_i, s_{i+1}) = v_0 + \tau[f(s_i) - \gamma f(s_{i+1})],$$

and

$$P = P(s_1, \ldots, s_N, v_1, \ldots, v_N, t) = P(\mathbf{s}, \mathbf{v}, t), \tag{6}$$

the Fokker-Planck equation reads [17]

$$\frac{\partial P}{\partial t} = \sum_{i=1}^{N} \left\{ -\frac{\partial}{\partial s_i} [\underbrace{(v_{i-1} - v_i)}_{=ds_i/dt} P] \right.$$

$$\left. -\frac{\partial}{\partial v_i} \left[\left(\underbrace{\frac{W(s_i, s_{i+1}) - v_i}{\tau}}_{=dv_i/dt - \xi_i} \right) P \right] + \frac{D}{2}\frac{\partial^2 P}{\partial v_i^2} \right\}, \tag{7}$$

where we assume periodic boundary conditions $v_{k+N}(t) = v_k(t)$ and $s_{k+N}(t) = s_k(t)$ for a onedimensional ring of length L with N particles on it. In the following, we will show that the *ansatz*

$$P(\mathbf{s}, \mathbf{v}) = P(s_1, \ldots, s_N, v_1, \ldots, v_N)$$

$$= \mathcal{N} \exp \left[-\sum_j \left(\frac{U(s_j)}{\theta} + Bs_j + \frac{(v_j - V)^2}{2\theta} \right) \right] \tag{8}$$

is a stationary solution of the above Fokker-Planck equation, if the parameters V and θ are properly chosen, and if the so-called interaction potential U is defined by

$$U(s_i) = \frac{1 + \gamma}{2} \int_0^{s_i} ds \, f(s). \tag{9}$$

In equation (8),

$$\mathcal{N} = \left[\int_0^\infty d^N s \int_{-\infty}^\infty d^N v \, P(\mathbf{s}, \mathbf{v}) \right]^{-1} \tag{10}$$

is the normalization constant, and the Lagrange parameter B is required to meet the constraint $\sum_i s_i = L$ determining the actual particle density. Moreover,

$$V(t) = \langle v_i \rangle = \int\limits_0^\infty d^N s \int\limits_{-\infty}^\infty d^N v \, v_i P(\mathbf{s}, \mathbf{v}, t) \qquad (11)$$

is the average velocity and

$$\theta(t) = \langle (v_i - V)^2 \rangle = \int\limits_0^\infty d^N s \int\limits_{-\infty}^\infty d^N v \, (v_i - V)^2 P(\mathbf{s}, \mathbf{v}, t)$$

$$(12)$$

the velocity variance. Notice that the stochastic model (3) and the corresponding Fokker-Planck equation (7) do not exclude negative velocities which is reflected by the integration limits in equations (11), (10), and (12). For all practical cases, however, the condition $\theta \ll V^2$ is valid which practically is compatible with non-negative velocities, cf. *ansatz* (8).

In the following, we will restrict our investigation to the stationary case with $dV/dt = 0$ and $d\theta/dt = 0$, which presupposes that the deterministic part of equation (3) fulfils the linear stability condition

$$(1 - \gamma)^2 \frac{df(L/N)}{ds} < \frac{1 + \gamma}{2\tau^2} \qquad (13)$$

(see Ref. [18] and the appendix for the method to determine this formula). Otherwise, dynamic patterns such as stop-and-go waves may emerge from the dissipative interactions of driven particles [6]. Notice that in the Hamiltonian case, $\gamma = 1$, the stability condition is always satisfied. Furthermore, the factorization assumption (8) requires that all variables s_i and v_i are statistically independent from each other. According to numerical simulation results, this is only the case if $(1 - \gamma)^2 df/ds$ is considerably smaller than the right-hand side of (13), i.e., the system is *far* from the instability point.

With the ansatz (8), the three terms of the Fokker-Planck equation (7) can be written as

$$-\sum_i \frac{\partial}{\partial s_i}[(v_{i-1} - v_i)P] = \sum_i (v_{i-1} - v_i)\left[\frac{1}{\theta}\frac{dU(s_i)}{ds_i} + B\right]P$$

$$= \sum_i (v_{i-1} - v_i)\left[\frac{(1+\gamma)f(s_i)}{2\theta} + B\right]P, \quad (14)$$

$$-\sum_i \frac{\partial}{\partial v_i}\left(\frac{W(s_i, s_{i+1}) - v_i}{\tau}P\right) =$$

$$\sum_i \frac{P}{\tau} - \sum_i \frac{W(s_i, s_{i+1}) - v_i}{\tau}\left[-\frac{(v_i - V)}{\theta}\right]P, \quad (15)$$

and

$$\sum_i \frac{D}{2}\frac{\partial^2 P}{\partial v_i{}^2} = \frac{D}{2}\sum_i \left[-\frac{1}{\theta} + \left(-\frac{v_i - V}{\theta}\right)^2\right]P. \qquad (16)$$

We will now use the fact that

$$\sum_i g_{i\pm 1}P = \sum_i g_i P \qquad (17)$$

for any i-dependent variable g_i, i.e. indices can be shifted because of the assumed periodic boundary conditions. In this way we find

$$\frac{\partial P}{\partial t} = \frac{1}{\theta}\sum_i \frac{1+\gamma}{2}(v_{i-1} - v_i)f(s_i)P + N\left(\frac{P}{\tau} - \frac{DP}{2\theta}\right)$$

$$+ \frac{1}{\theta}\sum_i \left[\frac{v_0 - v_i}{\tau} + f(s_i) - \gamma f(s_{i+1})\right](v_i - V)P$$

$$+ \frac{D}{2\theta^2}\sum_i (v_i - V)^2 P. \qquad (18)$$

Remarkably, this equation does not depend on the Lagrange parameter B anymore, which is needed to adjust to the particle density.

Note that ansatz (8) can only be a stationary solution with $\partial P/\partial t = 0$, if

$$\frac{1}{\theta} = \frac{2}{D\tau}. \qquad (19)$$

This relationship corresponds to the fluctuation-dissipation theorem of equilibrium thermodynamics. We point to the fact that this analogy breaks down if the factorization assumption (8) is no longer valid. Later on, we will show that this is the case if the system is not sufficiently far away from the regime of linear instability. Applying relation (19) also to the last term of equation (18) and using the decompositions $(v_{i-1} - v_i) = (v_{i-1} - V) - (v_i - V)$ and $(v_0 - v_i) = (v_0 - V) - (v_i - V)$, we find

$$\frac{\partial P}{\partial t} = \sum_i \frac{1-\gamma}{2\theta}(v_{i-1} + v_i - 2V)f(s_i)P$$

$$+ \frac{1}{\theta}\sum_i \frac{(v_0 - V)(v_i - V)}{\tau}P, \qquad (20)$$

and, with the factorization assumption (8) and shifting indices again according to (17), we obtain

$$\frac{\partial P}{\partial t} = \frac{1-\gamma}{\theta}\sum_i \left[f(s_i) + \frac{v_0 - V}{\tau}\right](v_i - V)P. \qquad (21)$$

We will distinguish the following cases:

1. In the case of a classical many-particle system with momentum conservation ($\gamma = 1$) and energy conservation, i.e. no dissipation ($\tau \to \infty$), we find $\partial P/\partial t = 0$, i.e. ansatz (8) is an exact stationary solution of the Fokker-Planck equation (7).

2. In the case of forwardly directed interactions as in vehicle traffic ($\gamma = 0$) and of vanishing correlations, we have

$$\lim_{N \to \infty} \frac{1}{N} \sum_i (v_i - V) \left[f(s_i) + \frac{v_0 - V}{\tau} \right] =$$

$$\left[\lim_{N \to \infty} \frac{1}{N} \sum_i (v_i - V) \right]$$

$$\times \left\{ \lim_{N \to \infty} \frac{1}{N} \sum_i \left[f(s_i) + \frac{v_0 - V}{\tau} \right] \right\}. \quad (22)$$

The first factor vanishes because of

$$V = \lim_{N \to \infty} \frac{1}{N} \sum_i v_i, \quad (23)$$

but the second factor disappears as well: dividing equation (3) by N and summing up over i gives

$$\frac{1}{N} \sum_i \frac{dv_i}{dt} = \frac{1}{N} \sum_i \frac{v_0 - v_i}{\tau} + \frac{1}{N} \sum_i f(s_i)$$

$$+ \frac{1}{N} \sum_i \xi_i(t). \quad (24)$$

In the limit $N \to \infty$ of large enough particle numbers N, the left-hand side converges to dV/dt, while the last term on the right-hand side converges to 0. In the assumed stationary case with $dV/dt = 0$ and using $v_0 - v_i = (v_0 - V) - (v_i - V)$, this implies

$$0 = \lim_{N \to \infty} \frac{1}{N} \sum_i \left[\frac{v_0 - v_i}{\tau} + f(s_i) \right]$$

$$= \lim_{N \to \infty} \frac{1}{N} \sum_i \left[\frac{v_0 - V}{\tau} + f(s_i) \right] \quad (25)$$

because of $\lim_{N \to \infty} \frac{1}{N} \sum_i v_i = V = \frac{1}{N} \sum_i V$.

We conclude that the factorisation ansatz (8) satisfies the Fokker-Planck equation (7) if either the momentum is conserved ($\gamma = 1$), or if the single-particle gaps and velocities are independent from each other. Note that, in order to arrive at this conclusion, the special form (9) for the interaction potential, particularly the prefactor $(1 + \gamma)/2$, is required.

2.2 Hamiltonian description

An alternative approach is the Hamiltonian description. For this purpose, let us investigate the quasi-Hamiltonian

$$\mathcal{H} = \mathcal{T} + \mathcal{V} = \sum_i \frac{(v_i - V)^2}{2} + \sum_i U(s_i), \quad (26)$$

where v_i is fluctuating according to equation (3), so that $\mathcal{H}$ is fluctuating as well. Nevertheless, one can derive the following relations:

$$\frac{d\mathcal{H}}{dt} = \frac{d\mathcal{T}}{dt} + \frac{d\mathcal{V}}{dt}$$

$$= \sum_i (v_i - V) \frac{dv_i}{dt} + \sum_i \frac{dU(s_i)}{ds_i}$$

$$\times \left(\frac{ds_i}{dx_i} \frac{dx_i}{dt} + \frac{ds_i}{dx_{i-1}} \frac{dx_{i-1}}{dt} \right)$$

$$= \sum_i (v_i - V) \frac{dv_i}{dt} + \sum_i \frac{1 + \gamma}{2} f(s_i)(v_{i-1} - v_i)$$

$$= \sum_i (v_i - V) \left(\frac{v_0 - v_i}{\tau} + f(s_i) - \gamma f(s_{i+1}) + \xi_i(t) \right)$$

$$+ \sum_i \frac{1 + \gamma}{2} f(s_i)(v_{i-1} - v_i)$$

$$= \sum_i \frac{1 - \gamma}{2} (v_i + v_{i-1} - 2V) f(s_i)$$

$$+ \sum_i \frac{(v_0 - V)(v_i - V)}{\tau}$$

$$- \sum_i \frac{(v_i - V)^2}{\tau} + \sum_i (v_i - V) \xi_i(t). \quad (27)$$

Notice that multiplicative stochastic expressions such as $v_i(t)\xi(t)$ must be be understood according to the the Stratonovich interpretation, which allows to apply the normal rules of calculus [17]. Comparing the above expression with equation (20) shows that

$$\frac{\partial P}{\partial t} = \frac{P}{\theta} \frac{d\mathcal{H}}{dt} + \frac{1}{\theta} \sum_i \left[\frac{(v_i - V)^2}{\tau} - (v_i - V)\xi_i(t) \right] P. \quad (28)$$

Correspondingly, if the distribution P is stationary ($\partial P / \partial t = 0$), we have

$$\frac{d\mathcal{H}}{dt} = \sum_i \left[(v_i - V)\xi_i(t) - \frac{(v_i - V)^2}{\tau} \right]$$

$$= \sum_i (v_i - V) \left(\xi_i(t) - \frac{v_i - V}{\tau} \right). \quad (29)$$

In order to investigate under which conditions the Hamiltonian is conserved in the statistical average, we will calculate $\left\langle \frac{d\mathcal{H}}{dt} \right\rangle$ for two different cases (where $\langle ... \rangle$ denotes the average over infinitely many realisations of the system dynamics):

1. In a conservative system with no fluctuations ($\xi_i(t) = 0 = D$) and no dissipation ($\tau \to \infty$), we have $d\mathcal{H}/dt = 0$, independently of whether the interactions are symmetric or forwardly directed.

2. For many-particle systems with fluctuation terms and dissipation, one can show

$$\langle \xi_i(v_i - V) \rangle = \left\langle \frac{1}{2} \frac{d(v_i - V)^2}{dt} \right\rangle - \frac{v_0 - V}{\tau} \langle v_i - V \rangle$$

$$+ \frac{1}{\tau} \langle (v_i - V)^2 \rangle$$

$$- \langle [f(s_i) - \gamma f(s_{i+1})](v_i - V) \rangle$$

$$= \frac{1}{2} \frac{d\theta}{dt} - \frac{v_0 - V}{\tau}(\langle v_i \rangle - V) + \frac{\theta}{\tau}$$

$$- \langle f(s_i) - \gamma f(s_{i+1}) \rangle (\langle v_i \rangle - V). \quad (30)$$

This can be found by multiplication of equation (3) with $(v_i - V)$ and calculation of the ensemble average, assuming the factorization ansatz (8). The first term on the right-hand side vanishes in the stationary state. The second and the fourth term vanish because of $\langle v_i \rangle = V$. Therefore,

$$\langle \xi_i(v_i - V) \rangle = \frac{\theta}{\tau}, \quad (31)$$

and, together with equation (29), we arrive at

$$\left\langle \frac{d\mathcal{H}}{dt} \right\rangle = \frac{1}{\tau} \left(N\theta - \sum_i (v_i - V)^2 \right) = 0. \quad (32)$$

That is, in the statistical average we have $d\mathcal{H}/dt = 0$. The same is expected for the average Hamiltonian per particle, $H_1 = \mathcal{H}/n$ of systems with many particles. In fact, simulations show that H_1 fluctuates with amplitudes $\propto 1/\sqrt{N}$, while the Hamiltonian $\mathcal{H}$ itself fluctuates with amplitudes $\propto \sqrt{N}$, which is consistent with equilibrium hydrodynamic systems. As a consequence, stationary driven dissipative systems behave Hamilton-like, even if the interactions are forwardly directed and Newton's law "actio = reactio" is violated. This is, why the Hamiltonian statistics

$$P(\mathbf{s}, \mathbf{v}) = \mathcal{N} e^{-\mathcal{H}/\theta} \quad (33)$$

(the canonical distribution) is an approximate stationary solution of our driven dissipative many-particle system. (It is approximate, because the factorization assumption (8) holds only, if the system is far enough away from instability points, i.e. if τ is sufficiently small.) Note that the contribution $\sum_i Bs_i = BL$ in equation (8) gives just a constant prefactor and can be absorbed into the normalization factor.

In conclusion, the equilibrium solution (8) of conservative many-particle systems is also a good approximation for the steady-state solutions ($\partial P/\partial t = 0$) of driven many-particle systems of kind (3) with asymmetrical interactions, driving and dissipation effects, if the system is large enough, i.e. $N \gg 1$, and if correlations between gaps, between velocities, and between velocities and gaps are not significant. (In the regime of linear instability and close to it, correlations may be considerable, as is known from stop-and-go waves. Furthermore, we expect that fluctuations become essential for small systems).

3 Application to stochastic traffic models

In this section, we will formulate the results of the previous section in a way that can be tested by means of simulating specific models on a computer.

3.1 Single-particle distributions

The factorization (8) can be written in the form

$$P(s_1, \ldots, s_N, v_1, \ldots, v_N) = \prod_{i=1}^N g(s_i) \prod_{j=1}^N h(v_j), \quad (34)$$

i.e., the statistics of the particles can be described by the single-particle gap distribution function

$$g(s) = A e^{-[U(s)/\theta + Bs]}, \quad (35)$$

and the single-particle velocity distribution

$$h(v) = \frac{1}{\sqrt{2\pi\theta}} e^{-(v-V)^2/(2\theta)}. \quad (36)$$

Here, A is a normalization constant, B a Lagrangian parameter ensuring the density constraint, V the average velocity, and θ the velocity variance. With the exception of θ, all quantities are dependent on the particle density ρ.

3.2 Gap distribution

The two constants A and B of the gap distribution (35) are determined by the normalization condition

$$\int_0^\infty ds\, g(s) = 1, \quad (37)$$

and the constraint that the average gap is equal to the inverse of the global density:

$$\int_0^\infty ds\, s\, g(s) = \frac{1}{\rho}. \quad (38)$$

Defining the integrals

$$I_0(B) = \int_0^\infty ds\, \exp\left[-\left(\frac{U(s)}{\theta} + Bs \right) \right],$$

$$I_1(B) = \int_0^\infty ds\, s \exp\left[-\left(\frac{U(s)}{\theta} + Bs \right) \right],$$

$$I_2(B) = \int_0^\infty ds\, s^2 \exp\left[-\left(\frac{U(s)}{\theta} + Bs \right) \right],$$

we get

$$A = \frac{1}{I_0(B)}. \quad (39)$$

For B, we find the transcendental equation

$$AI_1(B) = \frac{I_1(B)}{I_0(B)} = \frac{1}{\rho}. \tag{40}$$

Using Newton's method with the initial guess $B_0 = \rho + 1/\sigma_s$ with σ_s defined in equation (44), one obtains for the k-th iteration

$$B_{k+1} = B_k + \frac{I_0(I_1\rho - I_0)}{\rho(I_2 I_0 - I_1^2)}, \tag{41}$$

where the integrals on the right-hand side are evaluated at $B = B_k$. It turns out that this method converges within very few iterations, unless $U(s_e) = U(1/\rho) \gg \theta$. In this case, however, the second derivative $U''(s_e)$ of the effective potential (9) typically satisfies the condition

$$\frac{|U''(s_e)|}{\theta} = \frac{(1+\gamma)|f'(s_e)|}{D\tau} \gg \rho^2\,, \tag{42}$$

allowing an asymptotic expansion of (35) that eventually leads to a Gaussian gap distribution

$$\tilde{g}(s)_{|U''(s_e)|\gg\rho^2} = \frac{1}{\sqrt{2\pi}\sigma_s} e^{(s-s_e)^2/(2\sigma_s^2)} \tag{43}$$

with

$$\sigma_s^2 = \frac{D\tau}{(1+\gamma)f'(s_e)}. \tag{44}$$

According to numerical results, the ranges of applicability of (41) and (43) (generally) overlap, allowing a fast and robust solution.

3.3 Velocity distribution and kinetic energy

Equation (36) states that, regardless of the density, of the potential, and of the directions of the interactions, the single-particle velocity distribution is Gaussian. The expectation value is equal to the stationary velocity without fluctuating terms. Furthermore, the velocity variance satisfies an analog of the fluctuation-dissipation theorem (19), i.e., the energy of the velocity fluctuations around the stationary value V is given by

$$T = \frac{1}{2}\langle(v_i - V)^2\rangle = \frac{D\tau}{4}. \tag{45}$$

We finally note that all the results of this section are valid only under the condition that the factorisation ansatz (8) holds sufficiently well. In the next chapter, we will show that this requires the system to be far enough away from instabilities (otherwise spatio-temporal patterns such as stop-and-go waves may appear).

4 Results

In this section, we will show by means of computer simulations, that the main predictions (35), (36), and (45)

Table 1. Parameter values used in the simulations for the stochastic OVM given by the equations (3), (47), and (48).

Parameter	Value
Desired velocity v_0	$30\,\text{m/s}$
Velocity relaxation time τ	$0.2\,\text{s}$
Interaction length l_{int}	$20\,\text{m}$
Shape parameter β	0.5
Symmetry parameter γ	0 and 1
Fluctuating force D	$20\,\text{m}^2/\text{s}^3$
Density ρ	$12\,/\text{km}$ and $30\,/\text{km}$

are valid if the system is in a regime that is far enough away from any collective instability. In order to quantify this condition, we conclude from (13) that the system becomes linearly unstable if the relaxation time τ exceeds some critical value τ_c. Thus, τ controls the stability properties, which allows us to define the dimensionless reduced control parameter

$$r = \frac{\tau}{\tau_c}. \tag{46}$$

Note that $r = 0$ denotes maximum stability (no external driving force or infinitely fast relaxation), while the linear threshold is characterized by $r = 1$. In particular, in the momentum-conserving case $\gamma = 1$, we have always $r = 0$. The condition "far away from the instability point" can be quantified by the condition $r \ll 1$.

4.1 Selected models

In order to obtain a specific model, the interaction force of the stochastic differential equation (3) has to be specified. We will simulate two types of interaction forces that are based on (i) the optimal-velocity model, and (ii) on a power law.

4.1.1 Stochastic optimal-velocity model (sOVM)

In the *stochastic optimal-velocity model* (sOVM), the interaction force f is given by [9]

$$f_{\text{sOVM}}(s) = \frac{V_{\text{OVM}}(s) - v_0}{\tau}, \tag{47}$$

where we assume the optimal-velocity function

$$V_{\text{OVM}}(s) = \frac{v_0\left[\tanh\left(\frac{s}{l_{\text{int}}} - \beta\right) + \tanh(\beta)\right]}{1 + \tanh(\beta)}. \tag{48}$$

Table 1 summarizes the meaning of the model parameters and the values used in the simulations. Notice that the conventional optimal-velocity model of Bando et al. [19] is obtained for the special case $\gamma = 0$ and $D = 0$ in the equations (3) and (4), respectively.

The sOVM has the following properties: the expectation value of the velocity for stationary conditions is given by

$$V_{\text{sOVM}}(s) = v_0 + (1-\gamma)V_{\text{OVM}}(s). \tag{49}$$

Furthermore, the effective potential (9) can be calculated analytically, resulting in

$$U_{\text{sOVM}}(s) = U_0 \ln \left\{ 1 + \exp \left[-2 \left(\frac{s}{l_{\text{int}}} - \beta \right) \right] \right\}, \quad (50)$$

where the prefactor is given by

$$U_0 = \frac{(1+\gamma)v_0 l_{\text{int}}}{2\tau (1 + \tanh \beta)}. \quad (51)$$

The dynamics of this model becomes linearly unstable if the relaxation time exceeds the critical value τ_c given by

$$\tau_c(\rho) = \frac{1 + \gamma}{2(1-\gamma)^2 V'_{\text{OVM}}(1/\rho)}, \quad (52)$$

see equation (13). For the parameters specified in Table 1, $\gamma = 0$, and $\rho = 30/\text{km}$, the critical value is given by $\tau_c(\gamma = 0) = 1/(2V'_{\text{OVM}}(1/\rho)) = 1.51\,\text{s}$. This corresponds to $r = 0.132$, when the parameters of Table 1 are assumed.

4.1.2 Stochastic power law model (sPLM)

An alternative, more physics-oriented model assumes that the interaction forces obey a power law [7,8]:

$$f_{\text{sPLM}}(s) = -a_0 \left(\frac{l_{\text{int}}}{s} \right)^\delta, \quad (53)$$

which, together with (2) and (3), results in the stochastic power-law model (sPLM). The associated effective potential (9) is given by

$$U_{\text{sPLM}}(s) = \frac{(1+\gamma)a_0 l_{\text{int}}^\delta}{(\delta - 1)s^{\delta-1}}, \quad (54)$$

and the expectation value for the velocity is equal to

$$V_{\text{sPLM}}(s) = v_0 - (1-\gamma)\tau a_0 \left(\frac{l_{\text{int}}}{s} \right)^\delta. \quad (55)$$

This model differs qualitatively from the stochastic OVM in the following aspects:

- If $\gamma < 1$, the stationary velocity becomes zero for a finite average gap $s_e(V = 0) = [(1-\gamma)\tau a_0/v_0]^{1/\delta}$. In contrast, the stationary velocity of the sOVM for any $\gamma > 0$ is nonzero, even at maximum density, $s_e = 0$.
- The potential (54) of the stochastic power-law model diverges for $s \to 0$, while the potential (50) of the sOVM remains finite. For the chosen parameters and $\gamma = 0$, we have $U_{\text{sOVM}}(0) = U_0 \ln(2) = 1347\,\text{m}^2/\text{s}^2$. Consequently, any car approaching a standing vehicle with a velocity exceeding $\sqrt{2U_{\text{sOVM}}(0)} = 52\,\text{m/s}$ will lead to a rear-end collision. This velocity decreases with increasing values of τ, reaching $18.9\,\text{m/s}$ at the limit of linear stability. In contrast, no such collisions are possible in the stochastic power-law model. Nevertheless, this model can become linearly unstable as well.

4.2 Computer simulations

We have simulated a closed ring road of length $L = 9\,\text{km}$ for the sOVM, and $L = 40\,\text{km}$ for the sPLM. We have also simulated larger systems resulting in no significant differences. We have started the simulations with deterministic initial conditions $s_i = 1/\rho$, and $v_i = V(s_i)$, corresponding to a single-particle distribution function

$$P_1(s,v,0) = \delta \left(v - V\left(\frac{1}{\rho}\right) \right) \delta \left(s - \frac{1}{\rho} \right), \quad (56)$$

where $\delta(.)$ represents Dirac's delta function. Since this initial condition does not correspond to a stationary solution, we have run the simulations for a transient time of $72\,000$ s, before recording the results for further $36\,000$ s.

For the numerical update, we have applied the explicit scheme

$$v_i(t + \Delta t) = v_i(t) + a_i(t)\Delta t + z_t \sqrt{D\Delta t}, \quad (57)$$

$$x_i(t + \Delta t) = x_i(t) + \left[\frac{v_i(t) + v_i(t + \Delta t)}{2} \right] \Delta t, \quad (58)$$

where $a_i(t)$ denotes the deterministic part of the right-hand side of equation (3), and $z_t \sim N(0, 1)$ are independent realizations of a Gaussian distributed quantity with zero mean and unit variance.

The velocity update (57) corresponds to decomposing the deterministic and stochastic parts of the accelerations. While the deterministic part corresponds to an Euler update, the stochastic part is a result of explicitly solving the stochastic differential equation

$$\frac{dv_i^{(s)}}{dt'} = \xi_i(t')$$

for the initial conditions $v_i^{(s)}(t) = 0$ at time $t' = t$. The solutions $v_i^{(s)}(t + \Delta t) = \sqrt{D\Delta t}\, z_t$ are realizations of random-walk trajectories, which are Gaussian distributed with expectation value zero, and variance $D\Delta t$.

Notice that, for sufficiently small update times, this update scheme should converge (in the statistical sense) to the true solutions of (2) and (3). In the simulations, we have set $\Delta t = 0.04\,\text{s}$. To verify the convergence, we have also run some simulations with lower values of the time step (down to $\Delta t = 0.001\,\text{s}$) and found less than 1% deviation.

4.3 Gap distribution

Figure 1 shows the simulated gap distributions for the stochastic OVM for two densities and two values of the symmetry parameter γ. For comparatively low densities (Fig. 1a), both the predicted and the observed distributions are markedly asymmetric. Furthermore, the direction of interaction plays a role as well. For the limiting case of a car-following model ($\gamma = 0$), the gap distribution is
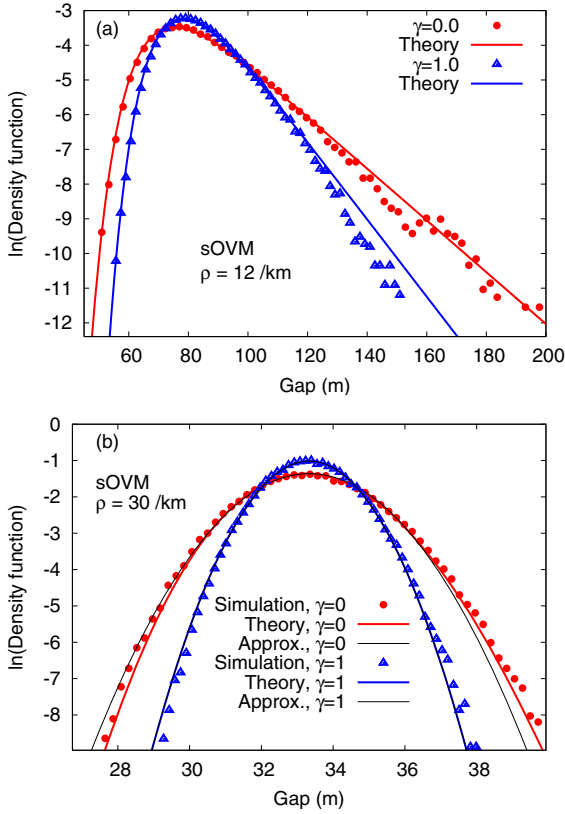
Fig. 1. (Color online) Stationary gap distributions for the stochastic optimal velocity model (sOVM) with the parameters specified in Table 1 on a ring road and densities (a) of $\rho = 12\,\mathrm{veh\,km}$, and (b) of $\rho = 30\,\mathrm{veh\,km}$. Plotted are the simulated data (symbols), the theoretical distribution (35) (thick solid line), and, for the higher density, the Gaussian approximations (43) (thin lines).

Table 2. Parameter values used in the simulations for the stochastic power-law model (3) and (53).

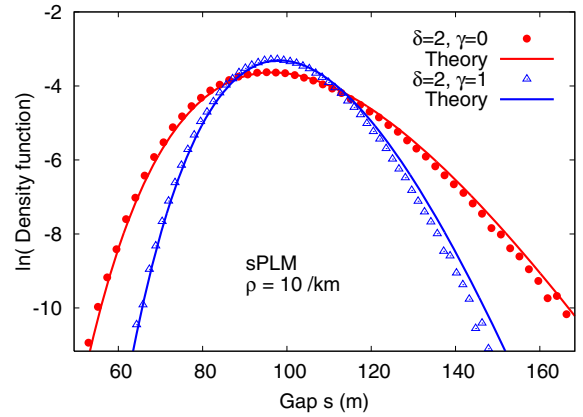| Parameter	Value
Desired velocity v_0	$30\,\mathrm{m/s}$
Velocity relaxation time τ	$2\,\mathrm{s}$
Interaction distance l_{int}	$20\,\mathrm{m}$
Acceleration a_0	$2\,\mathrm{m/s^2}$
Interaction exponent δ	2
Symmetry parameter γ	0 and 1
Fluctuating force D	$0.2\,\mathrm{m^2/s^3}$
Density ρ	$10\,\mathrm{/km}$

Fig. 2. (Color online) Stationary gap distributions for the stochastic power-law model (sPLM) with the parameter and simulation settings specified in Table 2.

wider than in the symmetric (momentum-conserving) case $\gamma = 1$. Generally, there is a good agreement between the theoretical expressions and the data. The only exception is the large-gap tail for symmetric forces at the lower density. In contrast, for the car-following case $\gamma = 0$, even the tails are reproduced correctly (within statistical fluctuations). The same agreement has been found for the higher density, irrespective of the value of γ. This is remarkable since additional assumptions have been necessary in Section 2 to derive the theoretical distributions for the car-following case. Consequently, one would expect larger errors compared to the isotropic case.

Now we investigate the influence of the densities on the form of the gap distribution. Comparing Figure 1a with Figure 1b, one may conclude that, when increasing the density, the distributions become more and more symmetric. Further simulations showed that the distribution becomes significantly asymmetric if the single-particle kinetic energy $T = D\tau/4$ exceeds the effective potential energy $U(1/\rho)$ by at last one order of magnitude. Specifically, for the situation of Figure 1, we have $T = 1\,\mathrm{m^2/s^2}$ for all values of ρ and γ, while the effective potential energy corresponding to plot (a) is given

by $U_{\mathrm{sOVM}} = (1 + \gamma)\,0.127\,\mathrm{m^2/s^2}$ and that of plot (b) by $U_{\mathrm{sOVM}} = (1 + \gamma)\,95.0\,\mathrm{m^2/s^2}$.

For sufficiently high densities, when the standard deviation of the gap distribution is much smaller than the average gap $1/\rho$, the Gaussian assumption (43) should become valid. To determine the range of validity, we plotted the Gaussian approximation in the relevant Figure 1b, in addition to the general distribution (35). For the case $\gamma = 1$ corresponding to $\sigma_s^2 = 1.21\,\mathrm{m^2}$, the Gaussian approximation agrees nearly perfectly with the full theoretical curve (the curves overlap with no visible difference). For $\gamma = 0$ ($\sigma_s^2 = 2.42\,\mathrm{m^2}$), however, a significant difference is found, but the distribution (35) already displays a significant skewness for this case. Further simulations showed that the Gaussian approximation is applicable whenever the full distribution (35) is sufficiently symmetric.

In order to evaluate the robustness of the predictions with respect to different model types, we have simulated the gap distributions for the stochastic power-law model as well. The results are shown in Figure 2. Apart from minor deviations at the large-gap tails, we found a remarkable agreement between theory and simulation. Moreover, the predicted distributions for the car-following case $\gamma = 0$ and the symmetric case $\gamma = 1$ are significantly different both with respect to variance and shape. This supports the particular specification (9) of the effective potential.
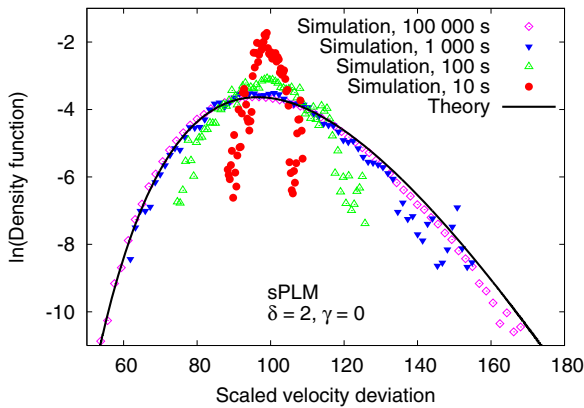
Fig. 3. (Color online) Relaxation of the (initially δ-shaped) gap distribution to its stationary distribution for the stochastic power-law model with the parameters specified in Table 2. The figure compares simulation results at different points in time (symbols) with the theoretical stationary distribution (solid line).

Finally, we looked closer at the relaxation dynamics of the initially δ-correlated distributions, see equation (56), towards the stationary distributions. A very slow relaxation could be a possible reason for the deviations found sometimes at the large-distance tails of the gap distributions. In Figure 3, we display snapshots of the evolution of the distribution for different simulation times. The results show that the relaxation time is considerable, particularly for low densities. Moreover, the relaxation process is particularly slow at the tails, so it may be a plausible reason for the remaining deviations.

4.4 Velocity distribution

In contrast to the gap distributions, the predicted velocity distributions are always Gaussian. Moreover, the velocity variance should satisfy the fluctuation-dissipation theorem (19). As a consequence, the variance may neither depend on the density nor on the direction of the interacting forces. Figure 4 shows simulated velocity distributions for the stochastic OVM at the higher density corresponding to Figure 1b. One observes that, with the exception of small but systematic deviations from the Gaussian shape for the car-following case $\gamma = 1$, all theoretical predictions are fulfilled. For the lower density $\rho = 12$ /km (not shown), the agreement was nearly perfect for all values of γ.

In contrast to the gap distributions, the agreement of the velocity distributions improves when going from the car-following to the conservative case and when decreasing the density. This can possibly be explained by the distance from the instability point, see equation (13). For the densities $\rho = 12$ /km and 30 /km, the dimensionless distances $r = \tau_c/\tau$ from the instability point are given by $r = 0.001$ and 0.132, respectively, while we have $r = 0$ for the conservative case. Obviously, the agreement increases with the degree to which the requirement $r \ll 1$ is satisfied.
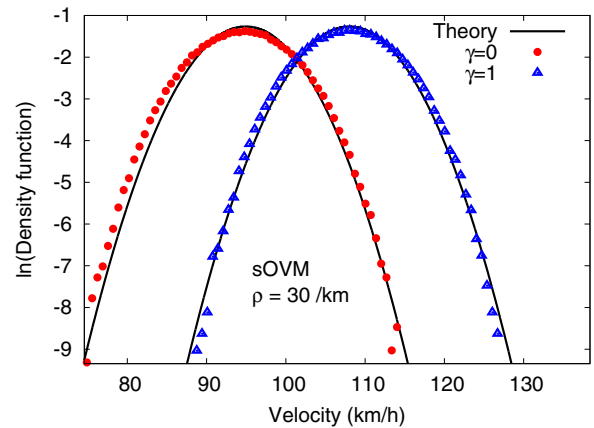

Fig. 4. (Color online) Stationary velocity distribution for the stochastic OVM with the parameters specified in Table 1.
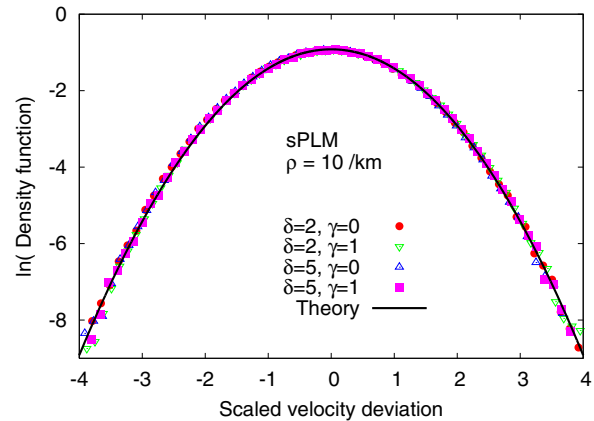

Fig. 5. (Color online) Stationary velocity distributions for the stochastic power-law model with the parameters specified in Table 2. The velocity distributions have been normalized with respect to the theoretical expectation value V, see equation (55), and the variance (19).

In Figure 5, we have plotted the simulated distributions for the stochastic power-law model for different values of the density and the symmetry parameter γ. In each simulation, we have normalized the distribution to the theoretical expectation value (55) and variance (19), so we expect that all curves should collapse onto each other in the ideal case. This collapse is, in fact, observed, thanks to values of r below 0.12 for all cases.

Finally, we investigate the relaxation process from the δ-correlated initial velocity distribution to the stationary distribution. Figure 6 shows that there is a significant scale separation for the relaxation times: while the typical velocity relaxation time scale is of the order of seconds, it is of the order of a hundred seconds for the gap distribution. After 1 000 s, even the tails of the velocity distribution are perfectly equilibrated, while for the gaps, this takes longer by a factor of more than one hundred.

We conclude that, in contrast to the case of gap distributions, long relaxation times cannot explain possible differences between the theoretical and simulated velocity
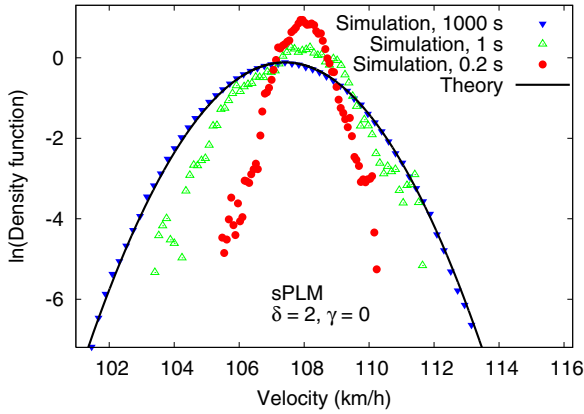
Fig. 6. (Color online) Relaxation of the velocity distribution to the Gaussian stationary distribution for the stochastic power-law model with the parameters specified in Table 2. Initially, all particles had the same gaps $s_i = 1/\rho$, and all velocities were equal to the expectation value. The figure compares simulation results at different points in time (symbols) with the theoretical stationary distribution (solid line).

distributions, as noticeable in Figure 4. These will be explained in the following.

4.5 Kinetic energy and correlations

One of the crucial assumption in the derivation of the gap and velocity distributions of Section 2 is the assumption of zero correlations, which requires that the system is far from any instability, i.e. $r \ll 1$. In classical thermodynamic systems, it is well known and theoretically understood [20] that the energy contained in the fluctuations increases near a phase transition, resulting in "critical opalescence" and other observable phenomena. The same has been found in driven thermodynamic systems such as Rayleigh-Bénard convection or electrohydrodynamic convection [21] below the deterministic threshold, which will be further discussed in Section 5.

It is therefore very interesting to investigate the stochastic properties of our driven particle-systems as a function of the distance from threshold, i.e., varying the relaxation time from $\tau = 0$ to $\tau = \tau_c$ or, equivalently, the control parameter from $r = 0$ to $r = 1$.

Figure 7 shows the single-particle kinetic energy of the fluctuations as a function of the relaxation time for several values of the directional parameter γ. The kinetic energy has been normalized to the value (45) resulting from the fluctuation-dissipation theorem (19). As in the physical systems mentioned above, we found significantly increased, so-called "critical fluctuations" near the linear threshold, which is located at $\tau_c = 1.51$ s for $\gamma = 0$ and at $\tau_c = 2.83$ s for $\gamma = 0.2$ while no such threshold exists for $\gamma = 1$.

Finally, we compared the observed increase factor of the fluctuation energy with the function $(1 - r)^{-0.5}$ of
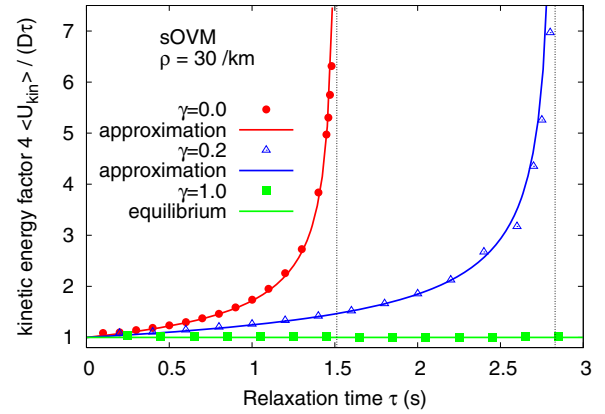

Fig. 7. (Color online) Average kinetic energy per particle for different values of the relaxation time and three values of the anisotropy parameter γ. The amplification of the velocity variance with growing values of τ reflects critical fluctuations close to the instability point, see equation (13). The energy has been plotted relative to the theoretical value corresponding to the fluctuation-dissipation theorem (symbols). The solid curves display the function $1/\sqrt{1-r}$ of the reduced control parameter r, see (46), and the thin vertical lines give the asymptotics for $\tau \to \tau_c$ ($r \to 1$).

the scaled distance to the threshold (scaled control parameter). The form is motivated by the observation that in many onedimensional physical systems, the scaling exponent of velocity fluctuations near threshold is equal to $\delta = -1/2$. The agreement was astonishing for all investigated values of r and γ, cf. Figure 7.

5 Conclusion

In this contribution, we have investigated the statistical properties of onedimensional dissipative driven many-particle systems violating the law "actio = reactio". Such systems can represent, for example, vehicular traffic or queuing systems with interactions.

In the theoretical derivation, we have shown that such systems show a Hamilton-like statistics when interparticle correlations play no significant role. The theoretical predictions were confirmed by simulations: without a single free parameter to fit, we quantitatively obtained the typical characteristic properties of Hamiltonian systems such as velocity and gap statistics corresponding to a canonical ensemble $\propto e^{-\mathcal{H}/\theta}$ when the Hamiltonian $\mathcal{H}$ contains the usual contributions of kinetic and potential energy as in physical Hamiltonian systems. Furthermore, the velocity variance satisfied the fluctuation-dissipation theorem. As only prerequisite, we have found that the system must be far away from any instability point. This is consistent with the theoretical requirement of vanishing correlations, since collective instabilities such as stop-and-go traffic correspond to highly correlated particles.

In the first moment, these results appear to be quite surprising. For example, in traffic systems neither energy

nor momentum are conserved during vehicle interactions, and the driving force keeps the system permanently far from equilibrium. While conservative systems conserve momentum and energy in each single interaction, in the driven dissipative systems studied by us, the additional relaxation term $(v_0 - v_i)/\tau$ causes the average velocity V to relax to the "free" or "desired" speed v_0.

However, even systems violating the law "actio=reactio" may be mapped to effectively conservative systems by a Galilei transformation. Defining velocities $u_i = v_i - V$ relative to the stationary velocity V, equation (3) becomes

$$\frac{du_i}{dt} = -\frac{u_i}{\tau} + f(s_i) - f(1/\rho) + \gamma\left[f(s_{i-1}) - f(1/\rho)\right]. \quad (59)$$

One sees that the constant terms $-f(1/\rho)$ and $\gamma f(1/\rho)$ resulting from the driving force and the relaxation dynamics supplement the interaction forces by counteracting forces – irrespective of the value of γ – such as in momentum-conserving systems.

One big difference of system not conserving momentum, however, remains when compared to conservative system: the conservative many-particle system always behaves dynamically stable, while the dissipative system potentially produces stop-and-go waves, when the linear stability condition (13) is not fulfilled. According to computer simulations, close to the instability point, the driven dissipative many-particle system tends to produce correlations between distances and velocities, and between successive particles [22].

This corresponds to pattern formation phenomena that would not occur in conservative systems. Such kinds of pattern formation phenomena have, for example, been investigated in fluid systems driven by thermal gradients (Rayleigh-Bénard convection), coriolis forces (Taylor-Couette flow), electrical fields (electroconvection), or concentration gradients (binary-mixture convection), see reference [21] for a review. Moreover, the increase of thermal fluctuations when approaching a linear stability threshold from below has been investigated theoretically and experimentally for the above systems [23–26]. Near the threshold, but in the regime of linear response, the fluctuations should increase according to a power law, where the scaling exponents depend on the dimensionality and symmetry classes of the systems [27]. Specifically, if the fluid systems are quasi-onedimensional, their fluctuations typically increase proportional to $(1 - r)^{-1/2}$ where the reduced control parameter r is defined in analogy to equation (46), with τ replaced by a suitable driving force such as voltage or a temperature gradient. Near the threshold, however, deviations have been observed empirically [28].

It appears that in our case the fluctuations scale proportionally to $1/\sqrt{1-r}$ as well. A theoretical foundation and a closer investigation of the above Fokker-Planck equation near the instability point and beyond will be subject of our future studies.

Appendix A: Derivation of the linear stability criterion (13)

The starting point of a linear stability analysis is the deterministic version of equations (2) and (3). For a given global density $\rho = 1/s_e$, its homogeneous-stationary solution is determined by

$$x_j(t) = j s_e + W_e t, \quad (60)$$

$$v_j(t) = W_e = W(s_e, s_e) = v_0 + \tau(1 - \gamma)f(s_e). \quad (61)$$

We expand equations (2) and (3) around this solution by introducing linear perturbations y_j and u_j via $x_{j+1} - x_j = s_e + y_j$ and $v_j = W_e + u_j$. Linearizing the resulting equations gives

$$\frac{dy_j}{dt} = u_{j+1} - u_j, \quad (62)$$

$$\frac{du_j}{dt} = \frac{-u_j}{\tau} + f'(s_e)(y_j - \gamma y_{j-1}). \quad (63)$$

Decomposing the linear perturbations into Fourier modes $y_j = \tilde{y}e^{ijk+\lambda t}$ and $u_j = \tilde{u}e^{ijk+\lambda t}$ leads to a homogeneous linear system of equations for the amplitudes $\tilde{y}$ and $\tilde{u}$. It is nontrivially solvable if the linear growth rate λ satisfies a characteristic quadratic equation. Its roots can be written as

$$\lambda_k^{(1,2)} = -\frac{1}{2\tau}\left[1 \pm \sqrt{1 - 4ab(1 - \cos k) - 4ia\sin k}\right], \quad (64)$$

where i is the imaginary unit, and

$$a = \tau^2 f'(s_e)(1 - \gamma), \quad (65)$$

$$b = \frac{1 + \gamma}{1 - \gamma}. \quad (66)$$

The system is linearly stable ("string stable"), if the real parts of the growth rates satisfy $\text{Re}\,(\lambda_k^{(1,2)}) < 1$ for all wave numbers $k \in]0, \pi]$ that are allowed by the system. After some intermediate steps (see Ref. [29]), this leads to the condition

$$a \sin^2 k \le b(1 - \cos k), \quad (67)$$

which is equivalent to $a < b/2$. Inserting the definitions (65) and (66) finally leads to the linear stability condition (13) in the main text.

References

1. T. Riethmüller, L. Schimanski-Geier, D. Rosenkranz, T. Pöschel, J. Stat. Phys. **86**, 421 (1997)
2. U. Erdmann, W. Ebeling, L. Schimansky-Geier, F. Schweitzer, Eur. Phys. J. B-Cond. Matter **15**, 105 (2000)
3. P. Reimann, R. Kawai, C. Van den Broeck, P. Haenggi, Europhys. Lett. **45**, 545 (1999)

4. R. Mahnke, J. Kaupužs, Phys. Rev. E **59**, 117 (1999)
5. R. Kühne, R. Mahnke, I. Lubashevsky, J. Kaupužs, Phys. Rev. E **65**, 66125 (2002)
6. D. Helbing, Rev. Mod. Phys. **73**, 1067 (2001)
7. D. Helbing, M. Treiber, eprint `arxiv:cond-mat/0307219` (2003)
8. M. Krbalek, D. Helbing, Physica A **333**, 370 (2004)
9. D. Helbing, M. Treiber, A. Kesting, Physica A **363**, 62 (2006)
10. M. Mehta, *Random Matrices* (Academic Press, 2004)
11. M. Krbalek, P. Šeba, P. Wagner, Phys. Rev. E **64**, 066119 (2001)
12. D.N. Zubarev, V.A. Morozov, G. Röpke, *Statistical Mechanics of Nonequilibrium Processes* (Akademie Verlag, Berlin, 1996+1997), Vols. 1, 2
13. K.L. Klimontovich, *Statistical Theory of Open Systems* (Kluwer Academic Publishers, Dordrecht, 1995)
14. W. Ebeling, I. Sokolov, *Statistical Thermodynamics and Stochastic Theory of Nonequilibrium Systems* (World Scientific, Singapore, 2005)
15. M. Krbálek, J. Phys. A: Mathematical and Theoretical **40**, 5813 (2007)
16. T. Antal, G.M. Schütz, Phys. Rev. E **62**, 83 (2000)
17. H. Risken, *The Fokker-Planck Equation*, 2nd edn. (Springer, Berlin, 1989)
18. D. Helbing, Eur. Phys. J. B, submitted (2008), e-print `http://arxiv.org/abs/0805.3402`
19. M. Bando, K. Hasebe, K. Nakanishi, A. Nakayama, A. Shibata, Y. Sugiyama, J. Phys. I France **5**, 1389 (1995)
20. L. Landau, E. Lifshitz, *Fluid Mechanics* (Addison Wesley, Reading, MA, 1959)
21. M. Cross, P. Hohenberg, Rev. Mod. Phys. **65**, 872 (1993)
22. A.A. Zaikin, L. Schimansky-Geier, Phys. Rev. E **58**, 4355 (1998)
23. I. Rehberg, S. Rasenat, M. de la Torre Juárez, W. Schöpf, F. Hörner, G. Ahlers, H.R. Brand, Phys. Rev. Lett. **67**, 596 (1991)
24. M. Wu, G. Ahlers, D. Cannell, Phys. Rev. Lett. **75**, 1743 (1995)
25. M. Treiber, Phys. Rev. E **53**, 577 (1996)
26. W. Schöpf, I. Rehberg, Journal of Fluid Mechanics Digital Archive **271**, 235 (2006)
27. M. Treiber, L. Kramer, Phys. Rev. E **49**, 3184 (1994)
28. M.A. Scherer, G. Ahlers, F. Hörner, I. Rehberg, Phys. Rev. Lett. **85**, 3754 (2000)
29. D. Helbing (2008), eprint `arxiv:physics/0805.3402`